

Scanning tunneling microscopy study of Si growth on a Si(111) $\sqrt{3}\times\sqrt{3}$ -B surface

A. V. Zotov

*Institut für Physik, Universität der Bundeswehr München, 85577 Neubiberg, Germany
and Institute of Automation and Control Processes, 690041 Vladivostok, Russia*

M. A. Kulakov,* B. Bullemer, and I. Eisele

Institut für Physik, Universität der Bundeswehr München, 85577 Neubiberg, Germany

(Received 21 August 1995; revised manuscript received 1 February 1996)

Scanning tunneling microscopy is used to study the growth of Si on a Si(111) $\sqrt{3}\times\sqrt{3}$ -B surface at Si coverages from submonolayer range up to a few monolayers and in the temperature range from 20 to 600 °C. Already at room temperature the deposited Si atoms are very mobile on the Si(111) $\sqrt{3}\times\sqrt{3}$ -B surface. As a result, the amorphous Si islands are formed, leaving the $\sqrt{3}\times\sqrt{3}$ reconstruction between islands intact. The dangling bond “bright” adatoms of the Si(111) $\sqrt{3}\times\sqrt{3}$ -B surface were found to be preferential sites for island nucleation. At temperatures of Si(111) epitaxy (≥ 400 °C) Si islands grow amorphously up to a certain critical size and then “crystallize” to form epitaxial islands. The structure on top of epitaxial Si islands is always $\sqrt{3}\times\sqrt{3}$, which suggests B segregation to the surface. The island shape (random below 600 °C and hexagonal at 600 °C) is considered to be governed by the structure and properties of the Si(111) $\sqrt{3}\times\sqrt{3}$ -B surface. [S0163-1829(96)05019-9]

I. INTRODUCTION

The Si(111) $\sqrt{3}\times\sqrt{3}$ -B surface phase is unique from many viewpoints. In contrast to the other group-III adsorbate Al-, In-, and Ga-induced $\sqrt{3}\times\sqrt{3}$ superstructures that contain adsorbate adatoms on top of the bulk-like terminated Si(111) surface,¹ the structure of the Si(111) $\sqrt{3}\times\sqrt{3}$ -B surface is built of B atoms in the fivefold-coordinated substitutional sites directly under silicon T_4 adatoms.²⁻⁴ Thus the outer surface of the Si(111) $\sqrt{3}\times\sqrt{3}$ -B phase contains Si adatoms only, much like the clean Si(111) 7×7 surface. However, the chemical properties of these two surfaces are known to differ drastically.⁵⁻⁹ The comparative studies of various adsorption and growth phenomena on these surfaces are believed to be valuable in revealing the parameters controlling these processes.

Epitaxial growth of Si on Si surfaces, on the other hand, is of great interest from both a technological and a scientific point of view and it has been the subject of numerous investigations. We would like to note only the recent scanning tunneling microscopy (STM) studies¹⁰⁻¹³ that have provided the detailed atomic scale information about nucleation and growth processes. To our knowledge, no STM results have been reported so far for the Si overgrowth on Si(111) $\sqrt{3}\times\sqrt{3}$ -B in spite of the discovery of several interesting specific effects occurring upon the Si/Si(111) $\sqrt{3}\times\sqrt{3}$ -B interface formation [e.g., preservation of the ordered reconstruction at the buried Si/Si(111) $\sqrt{3}\times\sqrt{3}$ -B interface,^{14, 15} growth of epitaxial Si film on Si(111) $\sqrt{3}\times\sqrt{3}$ -B with twinned orientation,¹⁶ and nearly complete electrical activation of B at the buried amorphous Si/Si(111) $\sqrt{3}\times\sqrt{3}$ -B interface.^{17, 18}]

In the present paper we report the results of a STM study of the Si overgrowth on the Si(111) $\sqrt{3}\times\sqrt{3}$ -B surface in the

temperature range 20–600 °C. The main attention has been paid to the regularities of Si island formation at the early stages of Si deposition. The results obtained are compared with known data for Si growth on the Si(111) 7×7 surface.

II. EXPERIMENT

The samples used in this study were Si bars (15 \times 4.5 \times 0.35 mm³) cut from 0.005 Ω cm B-doped Si(111) wafers. The details of the preparation procedure of the Si(111) $\sqrt{3}\times\sqrt{3}$ -B surface have been described elsewhere.¹⁹ In brief, as the first step, the samples were annealed at 1250 °C for 2 h to induce the accumulation of B at the surface and near-surface region up to the concentration corresponding to the Auger electron B-to-Si peak ratio of about 0.04. The final substrate preparation included heating at 1250 °C followed by slow cooling at a rate of about 1 °C/s. As a result, a well-ordered Si(111) $\sqrt{3}\times\sqrt{3}$ -B surface was produced, such as that shown in Fig. 1. The only structural defects present at the surface were the “bright” adatoms in concentrations of 3–8 %. These adatoms are known to correspond to the Si adatoms above the Si atoms that substitute for the B atoms in regular ($\sqrt{3}\times\sqrt{3}$) positions.⁷ Si was deposited from a resistively heated Si bar at a rate of about 0.2 monolayer (ML)/min [1 ML = 7.8×10^{14} cm⁻², the site density of the unreconstructed Si(111) plane]. During deposition the pressure was below 4×10^{-10} Torr. The deposited Si coverages were determined using STM images considering the shape, size, height, and number density of Si islands on the surface. The temperatures of the sample above 350 °C were monitored by an infrared pyrometer with an accuracy of ± 10 °C. The temperatures from 20 to 350 °C were estimated by extrapolating the heating current-temperature dependence to lower currents. The accuracy in the latter case was about ± 50 °C. The

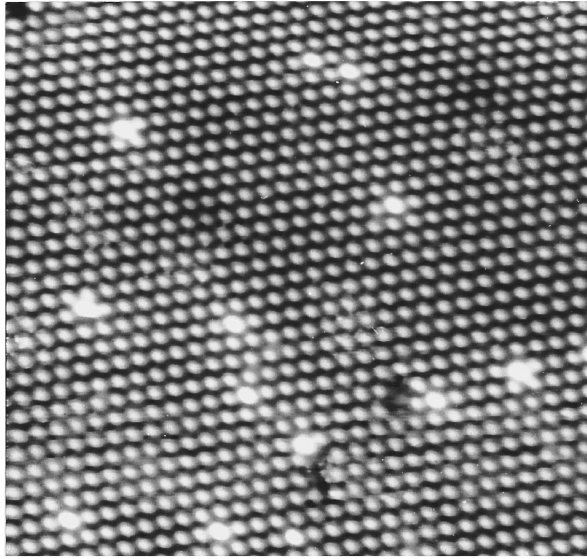


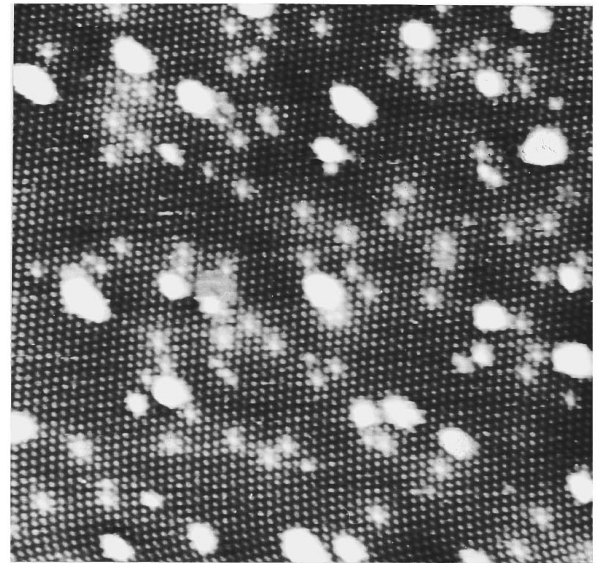
FIG. 1. $193 \times 193 \text{ \AA}^2$ STM image of the initial well-ordered Si(111) $\sqrt{3} \times \sqrt{3}$ -B surface obtained by annealing at $1250 \text{ }^\circ\text{C}$ followed by slow cooling.

STM observations were performed using standard Omicron apparatus driven by homemade electronics.²⁰ All the STM images presented here were obtained at a constant current of 0.2 nA and at sample biases of +1.2 to +2.4 V. Images are shown with a conventional gray scale keyed to the surface height.

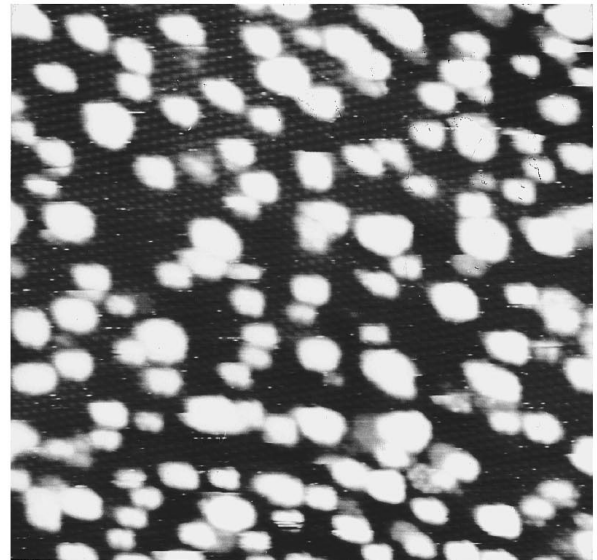
III. RESULTS AND DISCUSSION

A. Amorphous film growth

Figure 2 shows the STM images of the sample surface upon deposition of (a) 0.2 ML and (b) 1.5 ML of Si onto Si(111) $\sqrt{3} \times \sqrt{3}$ -B held at room temperature (RT). One can see that the film growth proceeds by the Volmer-Weber growth mechanism, i.e., via the formation of islands and leaving the $\sqrt{3} \times \sqrt{3}$ reconstruction between the islands intact. This implies that already at RT arriving Si adatoms migrate on the Si(111) $\sqrt{3} \times \sqrt{3}$ -B surface over relatively long distances. The migration distance of Si adatoms seems to depend not only on the Si adatom mobility but also on the surface density of bright Si adatoms of the initial Si(111) $\sqrt{3} \times \sqrt{3}$ -B surface. These adatoms are believed to trap the mobile Si adatoms and serve as island nucleation centers. There are several observations that support this assumption. (a) At the very early stages of Si deposition STM images of the majority of the bright adatoms become more bright (i.e., they are displayed as the higher protrusions), often losing their perfect round form. (b) The density of islands correlates with the density of the bright adatoms in the initial Si(111) $\sqrt{3} \times \sqrt{3}$ -B surface: the greater the density of the bright adatoms before Si deposition the greater island density upon Si deposition. (c) After a certain period of Si deposition no bright adatoms can be found at the Si(111) $\sqrt{3} \times \sqrt{3}$ -B surface between the islands. In addition, it should be noted that the dangling bond “restatoms” of the dimer-adatom-stacking fault structure have already been revealed as preferential sites for island nucleation at RT Si



(a)



(b)

FIG. 2. $385 \times 385 \text{ \AA}^2$ STM images showing Si island growth on Si(111) $\sqrt{3} \times \sqrt{3}$ -B at room temperature. The amount of Si deposited is 0.2 ML for (a) and 1.5 ML for (b).

growth on Si(111) 7×7 .¹⁰ So it is reasonable to assume that the dangling bond bright adatoms play the same role in case of the Si(111) $\sqrt{3} \times \sqrt{3}$ -B surface in which the overwhelming majority of adatoms (i.e., “dark” adatoms) are inert due to the charge transfer to the underlying substitutional B atoms.

The density of islands grows with Si deposition up to the dose at which the probability of Si adatom incorporation into existing islands starts to dominate over nucleation of the new islands. Recently, Mo *et al.*¹² have established a relationship between the surface diffusion coefficient of the adatoms and the number density of stable islands formed after submonolayer deposition in the “transient” regime in which new islands nucleate while coalescence and coarsening are not important. Using this relationship, we estimated the diffusion coefficient of a single Si atom on the Si(111) $\sqrt{3} \times \sqrt{3}$ -B surface to be about $10^{-11} \text{ cm}^2/\text{s}$ at RT. We would like to out-

line that this value is rather underestimated since the island nucleation is enhanced by the trapping of Si atoms by bright adatoms as discussed above. In any case, the value obtained is much greater than that for the 7×7 reconstructed Si(111) surface on which the migration of Si atom is limited at RT by an area of a half (7×7) unit cell¹⁰ and the diffusion coefficient of the order of 10^{-11} cm²/s would correspond to a temperature as high as 600 °C–700 °C.²¹ The detailed inspection of the Si islands did not reveal the presence of any ordered atomic structure and regions of uniform height within them, which suggests that all islands consist of amorphous Si.

The growth mode at 100 °C and 200 °C coincides with the one found at room temperature, i.e., the Si islands are amorphous and the island density is controlled initially by the density of the bright adatoms at the Si(111) $\sqrt{3}\times\sqrt{3}$ -B surface rather than by the growth temperature. Noticeable changes of the growth mode start at about 300 °C. At this temperature the island density becomes much less than at RT (at early stages the difference is about one order of magnitude) and the presence of bright adatoms does not produce a significant effect on the island nucleation. The estimated value of the surface diffusion coefficient for Si atoms at 300 °C is 2×10^{-8} cm²/s.²² The majority of the islands still have an amorphous structure.

B. Epitaxial film growth

The growth at 400 °C may be considered as the onset of Si epitaxy on the Si(111) $\sqrt{3}\times\sqrt{3}$ -B surface. Though at the early stages of growth the small islands look amorphous, after reaching a planar size of about 30–50 Å they become epitaxial. At greater Si exposures the growth of the new layer on the epitaxial islands starts also through accumulation of disordered silicon seen as cloudy structureless regions on their top close to the edges (Fig. 3).

The ordered structure on top of the islands is always $\sqrt{3}\times\sqrt{3}$, which suggests that B segregates from the Si:B substrate to the epitaxial Si islands. This STM observation (Si epitaxial growth is accompanied by B segregation at the lowest epitaxial temperatures) has significant implications for the fabrication of nanoscale δ -doped electronic devices. Recently, Headrick *et al.*¹⁴ have evidenced by means of grazing incidence x-ray diffraction the preservation of the B-induced $\sqrt{3}\times\sqrt{3}$ reconstruction under the Si cap layer. It has been outlined, however, that even at the lowest temperature for Si(111) epitaxy of about 400 °C, some boron disordering occurs and the epitaxial film remains defective.¹⁴ Our results imply that the δ -type structures formed suffer also from the outsmearing of the boron profile towards the surface.

If one compares the regularities of epitaxial island formation on Si(111) 7×7 and Si(111) $\sqrt{3}\times\sqrt{3}$ -B surfaces a clear difference becomes apparent. While in the case of Si growth on Si(111) 7×7 the island shape was reported to be triangular (with edges along $\langle 1\bar{1}0 \rangle$ directions) already at temperature of about 450 °C,¹⁰ the shape of the epitaxial Si islands on Si(111) $\sqrt{3}\times\sqrt{3}$ -B remains random (close to round and oval) up to 550 °C (Figs. 3 and 4). Only at growth temperatures as high as 600 °C do the relatively large islands become well-shaped hexagons with sides along the $\langle 11\bar{2} \rangle$ di-

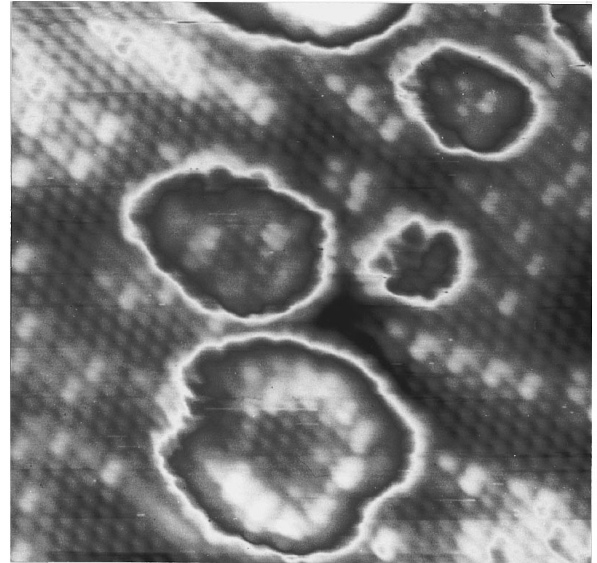


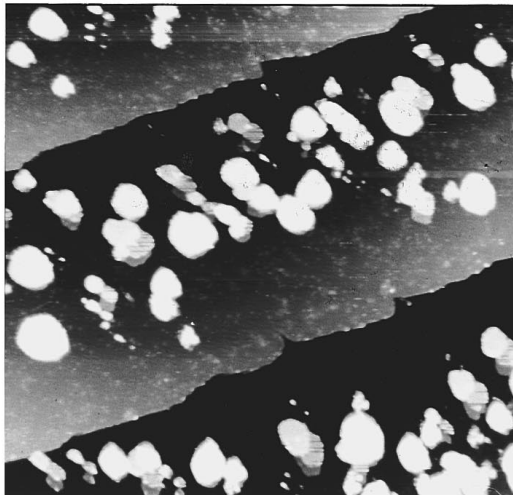
FIG. 3. Onset of epitaxial Si growth at a substrate temperature of 400 °C. The smaller islands have no apparent ordered structure, while larger ones are epitaxial. The cloudy bright areas on top of the epitaxial islands indicate that the formation of the new epitaxial layers is preceded by accumulation of amorphous Si. (Two individual full gray scales keyed to the substrate and to the epilayer are used to visualize atomic corrugations on both surface layers.)

rections (Fig. 5). The difference in island shape on these two surfaces seems to reflect the basic differences in their structure and properties, the Si(111) $\sqrt{3}\times\sqrt{3}$ -B surface being more isotropic and inert compared to the Si(111) 7×7 one.

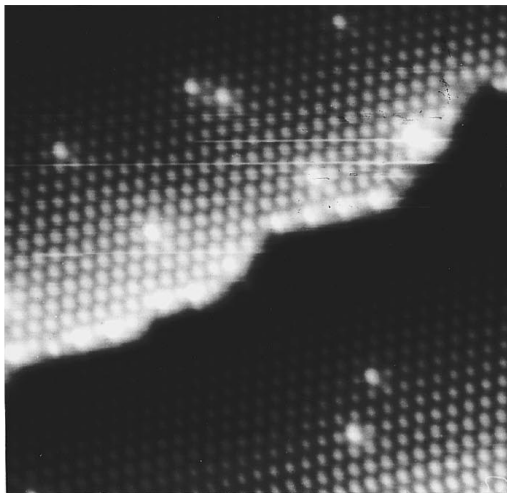
When the temperature is increased to 500 °C, the gradual changeover of the epitaxial growth mechanism becomes apparent, as evidenced by the large-scale STM image of Fig. 4(a). One now can see the presence of denuded zones near the step edges that are clearly asymmetric (the denuded zones at the top of the step are greater than at the bottom). This implies that simultaneously with the island formation, the growth through step propagation (i.e., according to the Frank–van der Merwe growth mechanism) sets in at this temperature. The high-resolution STM image of the step edge [Fig. 4(b)] shows that the integration of the Si atoms into the step edge proceeds by the formation of specific intermediate atomic structures. These structures have been repeatedly observed at many step edges and consist of bright oval-shaped elongated protrusions separated mainly by $2\sqrt{3}a_0$ [rarely by $3\sqrt{3}a_0$, where a_0 is the periodicity of the unreconstructed Si(111) surface] with some less distinct structural features between them. We assume tentatively that the nondistinct structures are formed by adatoms in the non-regular T_4 positions while oval protrusions correspond to Si-Si dimers.

IV. CONCLUSION

In conclusion, the initial stages of Si growth on the Si(111) $\sqrt{3}\times\sqrt{3}$ -B surface have been studied by scanning tunneling microscopy. The results obtained show that the specific structure and properties of the Si(111) $\sqrt{3}\times\sqrt{3}$ -B surface affect the Si growth mode, which differs essentially



(a)



(b)

FIG. 4. (a) $2055 \times 2055 \text{ \AA}^2$ STM image showing the epitaxial Si growth at $500 \text{ }^\circ\text{C}$. The presence of asymmetric denuded zones near the step edges indicates that island formation is now complemented by step motion epitaxial growth. (b) Step edge shown with higher magnification (the scale is $193 \times 193 \text{ \AA}^2$). Formation of specific intermediate structures at the step edge is apparent.

from the one on the clean $\text{Si}(111)7 \times 7$ surface in spite of the fact that the top layer of both surfaces contains Si adatoms only. The $\text{Si}(111)\sqrt{3} \times \sqrt{3}\text{-B}$ surface is known to be very inert (in the ideal case it has no dangling bonds). This inertness has important implications for Si growth: The deposited Si atoms are very mobile on this surface and already at room

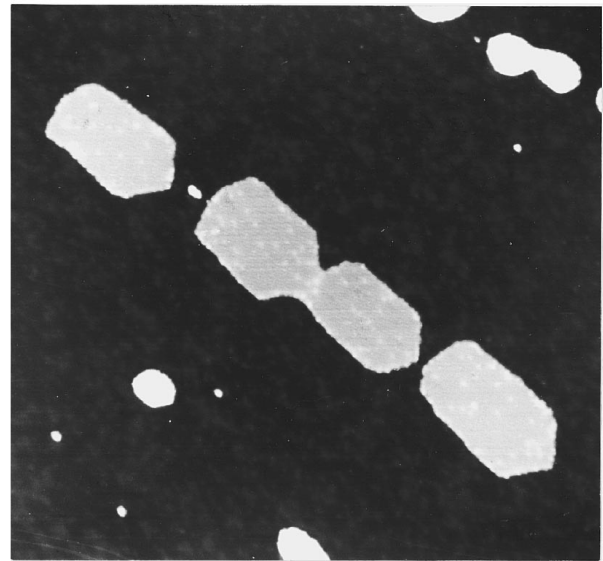


FIG. 5. Hexagon-shaped epitaxial Si islands grown on the $\text{Si}(111)\sqrt{3} \times \sqrt{3}\text{-B}$ surface at $600 \text{ }^\circ\text{C}$. The scale is $1930 \times 1930 \text{ \AA}^2$.

temperature Si film growth proceeds via island formation with a relatively small island number density leaving $\sqrt{3} \times \sqrt{3}$ reconstruction between the islands intact. The dangling bond bright adatoms, which are essentially the structural defects of the $\text{Si}(111)\sqrt{3} \times \sqrt{3}\text{-B}$ surface caused by substitution of B by Si, serve as preferential sites for island nucleation. Compared to the $\text{Si}(111)7 \times 7$ surface, the $\text{Si}(111)\sqrt{3} \times \sqrt{3}\text{-B}$ surface has a much weaker alignment effect on the deposited Si film. As a result, at temperatures of epitaxial growth (above about $400 \text{ }^\circ\text{C}$) islands grow amor- phously up to a certain critical size and become crystalline only after the formation of a sufficiently extended area of the $\text{Si}/\text{Si}(111)\sqrt{3} \times \sqrt{3}\text{-B}$ interface. The structure on top of epitaxial Si islands is always $\sqrt{3} \times \sqrt{3}$, which suggests that boron segregates from the substrate to the islands. The shape of epitaxial islands remains random up to about $550 \text{ }^\circ\text{C}$. The large islands grown at $600 \text{ }^\circ\text{C}$ have a hexagonal shape with edges along the $\langle 11\bar{2} \rangle$ directions, in accordance with the symmetry of the $\text{Si}(111)\sqrt{3} \times \sqrt{3}\text{-B}$ surface.

ACKNOWLEDGMENT

One of the authors (A.V.Z.) acknowledges the Alexander von Humboldt Foundation for financial support.

* Author to whom correspondence should be addressed. FAX: +49 89 60043560. Electronic address: e91bzeus@rz.unibw-muenchen.de

¹V.G. Lifshits, A.A. Saranin, and A.V. Zotov, *Surface Phases on Silicon. Preparation, Structure and Properties* (Wiley, Chichester, 1994).

²P. Bedrossian, R.D. Meade, K. Mortensen, D.M. Chen, J.A. Golovchenko, and D. Vanderbilt, *Phys. Rev. Lett.* **63**, 1257 (1989).

³I.W. Lyo, E. Kaxiras, and Ph. Avouris, *Phys. Rev. Lett.* **63**, 1261 (1989).

⁴R.L. Headrick, I.K. Robinson, E. Vlieg, and L.C. Feldman, *Phys. Rev. Lett.* **63**, 1253 (1989).

⁵P.J. Chen, M.L. Colaianni, and J.T. Yates, Jr., *J. Appl. Phys.* **70**, 2954 (1991).

⁶F. Bozso and Ph. Avouris, *Phys. Rev. B* **44**, 9129 (1991).

⁷Ph. Avouris, I.W. Lyo, F. Bozso, and E. Kaxiras, *J. Vac. Sci. Technol. A* **8**, 3405 (1990).

- ⁸Ph. Mathiez, T.P. Roge, Ph. Dumas, and F. Salvan, *Appl. Surf. Sci.* **56/58**, 551 (1992).
- ⁹Y. Taguchi, M. Daté, N. Takagi, T. Aruga, and M. Nishijima, *Appl. Surf. Sci.* **82/83**, 434 (1994).
- ¹⁰U. Köhler, J.E. Demuth, and R.J. Hamers, *J. Vac. Sci. Technol. A* **7**, 2860 (1989).
- ¹¹Y.-W. Mo, R. Kariotis, B.S. Swatzentruber, M.B. Webb, and M.G. Lagally, *J. Vac. Sci. Technol. A* **8**, 201 (1990).
- ¹²Y.-W. Mo, J. Kleiner, M.B. Webb, and M.G. Lagally, *Surf. Sci.* **268**, 275 (1992).
- ¹³Y. Shigeta, J. Endo, and K. Maki, *Phys. Rev. B* **51**, 2021 (1995).
- ¹⁴R.L. Headrick, B.E. Weir, A.F.J. Levi, B. Freer, J. Bevk, and L.C. Feldman, *J. Vac. Sci. Technol. A* **9**, 2269 (1991).
- ¹⁵K. Akimoto, I. Hirose, T. Tatsumi, H. Hirayama, J. Mizuki, and J. Matsui, *Appl. Phys. Lett.* **56**, 1225 (1990).
- ¹⁶R.L. Headrick, B.E. Weir, J. Bevk, B.S. Freer, D.J. Eaglesham, and L.C. Feldman, *Phys. Rev. Lett.* **65**, 1128 (1990).
- ¹⁷R.L. Headrick, A.F.J. Levi, H.S. Luftman, J. Kovalchik, and L.C. Feldman, *Phys. Rev. B* **43**, 14 711 (1991).
- ¹⁸A.V. Zotov, F. Wittmann, J. Lechner, I. Eisele, S.V. Ryzhkov, and V.G. Lifshits, *Appl. Phys. Lett.* **67**, 611 (1995).
- ¹⁹A.V. Zotov, M.A. Kulakov, S.V. Ryzhkov, A.A. Saranin, V.G. Lifshits, B. Bullemer, and I. Eisele, *Surf. Sci.* **345**, 313 (1996).
- ²⁰P. Heuell, S. Cuzdi, M.A. Kulakov, and B. Bullemer, *Thin Solid Films* **264**, 264 (1995).
- ²¹P.M. Agrawal, D.L. Thompson, and L.M. Raff, *J. Chem. Phys.* **91**, 6463 (1989).
- ²²Our data obtained at several growth temperatures provide a formal basis for determination of the activation energy and prefactor for diffusion. However, we believe that the values obtained should be erroneous due to the temperature-dependent effect of the preferred island nucleation on “bright” adatoms as well as due to the uncertainties in the growth temperatures we had in this experiment.